ELSEVIER

International Journal of Mass Spectrometry 182/183 (1999) 13–22

International Journal of Mass Spectrometry

Calculated energy barriers for the identity S_N2 reaction $H_2O + CH_3OH_2^+ \rightarrow {}^+H_2OCH_3 + OH_2$ in the gas phase, in water clusters, and in aqueous solution

Einar Uggerud

Department of Chemistry, University of Oslo, P. O. Box 1033 Blindern, N-0315 Oslo, Norway

Received 7 July 1998; accepted 16 September 1998

Abstract

The bimolecular nucleophilic substitution reaction $\mathbf{H_2O} + CH_3OH_2^+ \rightarrow {}^+\mathbf{H_2O}CH_3 + OH_2$ has been studied using various quantum chemical methods. Accurate barriers for the reaction in the gas phase are presented and discussed. The effect of microsolvation by water molecules in small clusters has been investigated. Extrapolation of the barrier obtained in the small clusters, using a linear relationship between the activation energy and the proton affinity of water clusters, gives a barrier for the reaction in aqueous solution which is in good agreement with that obtained in separate model calculations (polarized continuum model of a super molecule with the first solvation shell included). (Int J Mass Spectrom 182/183 (1999) 13–22)

Keywords: Energy barriers; $H_2O + CH_3OH_2^+ \rightarrow {}^+H_2OCH_3 + OH_2$; S_N2 reaction

1. Introduction

The chemical and physical properties of a molecule depend intimately on its surroundings. The rates and dynamical features of a chemical reaction are consequently strongly affected by the environment. An exothermic or thermoneutral ion-molecule reaction in the gas phase, if not hindered by energetic or entropic barriers for the chemical transformation, takes place with a rate constant close to the collision rate [1–3], which typically is of the order of $k_{coll} \approx 10^{-9}$ cm^3 mol^{-1} s^{-1}. The high efficiency of ion-molecule capture is because of the long range ion/induced-dipole interaction potential, which in vacuo has an r^{-4} dependence with respect to the separation, r, between the ion and the neutral molecule. Upon immersion into a solvent the behaviour of the reaction system changes dramatically. Unless the neutral reactant is the solvent, the long-range interaction potential is effectively screened by the bulk solvent. In consequence, the reactants tumble around among the solvent molecules for an extended period of time before they approach each other, thereby often making the process of molecular diffusion the rate determining step. Another noticeable difference is that in solution the surroundings provide a continuous heat bath for the reaction all the way from reactants to products, while the energy of a reacting system in the gas phase is conserved from the moment the reactants start to approach each other. In addition, the molecular properties of the reactants, intermediates and transition states are affected differently by the solvent [4,5].

Dedicated to the memory of Ben S. Freiser (1951–1997), a good friend and a gifted scientist.

1387-3806/99/$20.00
PII S1387-3806(98)14226-4

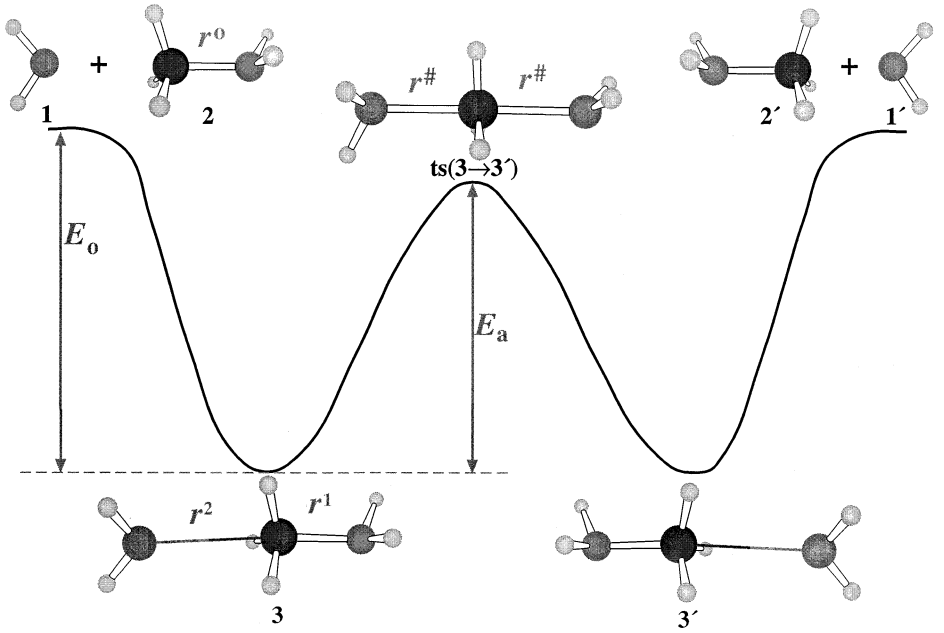

Fig. 1. Schematic potential energy diagram which defines some of the most important structural and energetical parameters used in the text.

This means that the barrier height for the actual chemical transformation depends on the nature of the medium.

Molecular clusters, [M] S_n, consisting of a variable number (n) of solvent molecules, S, plus the molecule of interest, M, provide the connection between the isolated gas phase molecule M(g) and that in the bulk liquid, M(solvent). It is of fundamental importance to study how the properties of clusters of this type change with the number of solvent molecules. For this purpose it is interesting to see if the chemical properties change gradually with cluster size, and if it is possible to extrapolate the behaviour in the solvent from that in small clusters.

We have recently studied reactions between water and different protonated alcohols in the gas phase by Fourier transform ion cyclotron resonance (FTICR) mass spectrometry [6]. Using isotopically labelled water we were able to determine the rate constant for the reaction:

$$H_2{}^{18}O + CH_3{}^{16}OH_2^+ \rightarrow {}^+H_2{}^{18}OCH_3 + {}^{16}OH_2 \quad (1)$$

to be $k_1 = 2.2 \times 10^{-13}$ cm^3 mol^{-1} s^{-1}. Application of ion-molecule collision theory shows that approximately only 1 out of 10 000 collisions results in reaction, implying a substantial barrier or bottleneck for the reaction. This was confirmed by an accompanying MP2/6-31G(d) quantum chemical model, which shows that a symmetrical transition structure of the type $[H_2O \cdots CH_3 \cdots OH_2]^+$ must be passed in order to complete the reaction. It turns out that the reaction has all the characteristics of a prototype S_N2 reaction. We employed microcanonical variational transition state theory (μ-VTST) to model the reaction kinetics. Necessary vibrational frequencies and rotational moments were taken from the quantum chemical calculation, and the rate constant was obtained as a function of the energy difference $\Delta E = E_a - E_0$ (Fig. 1). A value of $\Delta E = -13$ kJ mol^{-1} was obtained from the experimental rate constant. This means that the potential energy of the transition structure (including zero point vibration) is below that of the separated reactants. If the assumptions inherent in our μ-VTST calculations are correct,

this numerical estimate is accurate within a few kJ mol^{-1}.

In this article we will focus on some topics not covered in the previous article, to which it therefore represents an important extension. These topics are: (1) By subjecting the system to "benchmark" ab initio quantum chemical calculations we may be able to test the validity of the assumptions underlying our previous variational transition state calculation. Furthermore, we will examine the accuracy of more economical quantum chemical procedures, by comparing them with the results of the "benchmark" calculations. (2) Gradual addition of water molecules to the reaction system leads to a situation which eventually becomes the fully solvated case. We want to investigate how the barrier height changes in successively larger clusters, also using quantum chemical methods. In the limit the solvent may either be represented by an infinite number of water molecules, or by a structureless dielectric medium. By applying a so-called self consistent reaction field method on a medium sized cluster we attempt to give a realistic model of the solvent state.

2. Methods

Quantum chemical calculations were carried out using the program system GAUSSIAN94 [7]. Atomic basis sets were taken from this package as described in the following using standard nomenclature, e.g. 6-31G(d). Different quantum chemical methods were used, ranging from Hartree–Fock (HF) [8] and a hybrid density functional theory method according to Becke (B3LYP) [9], up to coupled cluster theory [10] at a very high level, CCSD(T). The abbreviation MP2 stands for Møller-Plesset perturbation theory [11] to second order, and QCISD [12] is quadratic configuration interaction taking single and double excitations into account. Unless otherwise noted, the MP2 calculations were done by omitting the core electrons from correlation (frozen core, FC). All relevant critical points (reactants, transition structures, intermediates and products) of the potential energy surface were characterized by complete optimization of the molecular geometries for HF/6-31G(d), B3LYP/6-31G(d), MP2/6-31G(d), MP2/6-31G(d,p) and QCISD/6-31G(d,p). Geometry optimization for the clusters was conducted with MP2/6-31G(d) only.

The respective single point energies were computed at these geometries as indicated. Harmonic frequencies were obtained by diagonalizing the mass-weighed Cartesian force constant matrix, calculated from the analytical second derivatives of the total energy (the Hessian). Harmonic frequencies obtained in this manner were used to calculate the zero point vibrational energies (zpve) as described below. All total energies reported include the zero point vibrational energies scaled by the factors of 0.9135 (HF/6-31G(d)), 0.9670 (MP2/6-31G(d)) and 0.9806 (B3LYP/6-31G(d)) [13]. For the G2 method [14] the built-in scale factor was used.

The self-consistent reaction field method used here (polarized continuum model, PCM) treats the surroundings as a polarizable continuum. The PCM method was originally developed by Miertus, Scrocco, Tomasi [15] and Miertus, Tomasi [16] and is included in GAUSSIAN94. It represents an extension of the Onsager model, and the molecule is placed in a cavity in the continuum. The cavity is constructed by overlapping spheres (each described by 98 data points) centered on the atoms of the molecule. The built-in radii (H: 1.2 Å, C: 1.5 Å, O: 1.4 Å) were used. A dielectric constant, $\varepsilon = 78.5$, for the surrounding medium was adopted.

3. Results and discussion

3.1. Gas phase

Association between water (**1**) and protonated methanol (**2**) leads to the complex $H_2O \cdots CH_3OH_2^+$ (**3**). This complex is the direct precursor for the transition structure, **ts(3 → 3′)**, for the actual chemical transformation. A minimum energy reaction path connects **ts(3 → 3′)** and the complex **3** on one side, and its mirror image **3′** on the other. This is depicted in Fig. 1. The global minimum of the potential energy surface (PES) is the hydrogen bonded complex

$CH_3OH_2^+ \cdots OH_2$. This complex is not included here, but is described in detail in the previous article [6]. It is approximately 70 kJ mol^{-1} lower in potential energy than **3**.

The intermolecular force in complex **3** is mainly of noncovalent nature (electrostatic and ion/induced-dipole terms). Despite this we notice a slight perturbation in the electron density of the $CH_3OH_2^+$ moiety which is reflected in the fact that $\mathbf{r}^1 > \mathbf{r}^0$ by more than 0.02 Å (Fig. 1 and Table 1). The interaction energy, E_0, is, depending on the quantum chemical procedure, in the range 41.0–50.2 kJ mol^{-1}. The very accurate CCSD(T) calculation provides the "benchmark" which all the other calculations are measured against. It turns out that the geometries are consistent through the series, and that they are well reproduced even with the simple HF and B3LYP schemes. The variation in the interaction energy, E_0, shows, not unexpectedly, that both the level of electron correlation and the basis set are crucial factors in obtaining accurate energy parameters for weakly bonded species. The relatively economical, but accurate G2 method performs quite well in this respect.

The calculated geometries of the transition structures show some more variation, but they are still surprisingly consistent. The difference between the largest (HF/6-31G(d)) and the smallest (MP2/6-31G(d)) $r^{\#}$ value is only 0.05 Å. The curvature along the reaction coordinate, expressed by the corresponding imaginary frequency of vibration, $v^{\#}$, is clearly more method dependent. The transition structure, **ts(3 → 3′)**, is of C_2 symmetry, with a symmetrical arrangement of a methyl between two water molecules. The reaction coordinate corresponds to an antisymmetric normal mode of vibration in which the displacements of the two water molecules are opposite to that of the methyl. Motion along the reaction coordinate from the **ts(3 → 3′)** to the structures **3** and **3′**, respectively, corresponds to a Jahn-Teller distortion from an unstable symmetric species.

The calculated potential energy barrier height, E_a, and thereby the energy difference ΔE, are seen to vary quite strongly with the quality of the wave function/density functional. In fact, the "benchmark" CCSD(T) calculation predicts the barrier to be almost

Table 1
Results of the quantum chemical calculations for $H_2O + CH_3OH_2^+ \rightarrow H_2O \cdots CH_3OH_2^+$ (complex) $\rightarrow \{H_2O \cdots CH_3 \cdots OH_2^+\}^{\#}$ (TS) → products

Method	Reactant energy Hartrees	Complex energy Hartrees	TS energy Hartrees	r^0 Å	r^1 Å	r^2 Å	$r^{\#}$ Å	$v^{\#}$ $\mathbf{i} \cdot cm^{-1}$	E_0 kJ mol^{-1}	E_a kJ mol^{-1}	ΔE kJ mol^{-1}
B3LYP/6-31G(d)	−192.340 86	−192.359 61	−192.349 61	1.522	1.553	2.597	1.974	363	49.3	26.3	−23.0
HF/6-31G(d)	−191.266 14	−191.283 24	−191.271 63	1.511	1.538	2.690	2.039	369	44.9	30.5	−14.4
MP2/6-31G(d)//HF/6-31G(d)	−191.756 65[a]	−191.775 69[a]	−191.758 66[a]	...	...	...	...	...	50.0	44.7	−5.3
MP2/6-31G(d)	−191.758 64	−191.777 75	−191.761 52	1.518	1.542	2.616	1.953	499	50.2	42.6	−7.6
MP2/6-31G(d,p)	−191.824 17	−191.842 98	−191.826 59	1.512	1.535	2.609	1.952	501	49.4	43.1	−6.3
QCISD/6-31G(d,p)	−191.859 16[b]	−191.877 53[b]	−191.861 96[b]	1.517	1.541	2.622	1.976	...	48.3	40.9	−7.4
G2 (0 K)[c]	−192.152 26[c]	−192.167 85[c]	−192.152 54[c]	1.516	1.539	2.614	1.952	369[c]	41.0	40.2	−0.8
MP2/6-311+G(2df,2pd)//MP2/6-31G(d,p)	−192.112 03[b]	−192.127 69[b]	−192.108 84[b]	...	...	...	...	...	41.1	49.5	8.4
CCSD(T)/6-311+G(2df,2pd)//MP2/6-31G(d,p)	−192.162 66[b]	−192.178 42	−192.160 91	...	...	...	...	...	41.4	46.0	4.6
CCSD(T)/6-311+G(2df,2pd)//QCISD/6-31G(d,p)	−192.162 67[b]	−192.178 45[b]	−192.160 93[b]	...	...	...	...	...	41.5	46.0	4.5

The total energies of the reactant, complex and the TS include appropriately scaled zero point vibrational energies (zpve).
[a] Zpve from HF/6-31G(d,p) optimized structure
[b] Zpve from MP2/6-31G(d,p) optimized structure
[c] In this composite procedure the geometry is optimized with MP2 = FULL/6-31G(d) which is used in a series of subsequent higher level calculations. Frequencies are calculated in a separate HF/6-31G(d) optimization step [12].

twice that for B3LYP. Comparison between the HF and MP2 calculations shows that neglect of electron correlation results in a quite significant underestimate of the barrier height. This stems from the tighter spatial requirements for the two C–O bond electrons in the complex, than for the corresponding two electrons of the prolate symmetrical HOMO (it stretches out from the $O\cdots C\cdots O$ axis) of the transition structure. The complex is consequently lowered more upon inclusion of electron correlation than the transition structure. The basis set is also of importance. This is demonstrated by comparing the MP2/6-311+G(2df,2pd) and the MP2/6 - 31G values. With the large 6-311+G(2df,2pd) basis set the correlation energy difference in E_a is slightly overestimated by MP2 compared to CCSD(T). The small differences in the QCISD/6-31G(d,p) and MP2/6-31G(d,p) geometries do not affect the outcome of the CCSD(T) calculations noticeably. This gives us confidence in the consistency of the geometries and thereby the accuracy of our "benchmark."

In the Introduction, we referred to our estimate of the energy difference of, $\Delta E = -13$ kJ mol^{-1}, which is based on our measured rate constant. Apparently, the HF/6-31G(d) value gives the best fit. The "benchmark" quantum chemical value differs by 18 kJ mol^{-1}. We must, however, take into account that the estimate was made indirectly using μ-VTST, and may therefore be the victim of inherent methodological problems. Several assumptions were made for the μ-VTST calculations. It was assumed that there is no hindrance of free passage between the two structures $H_2O\cdots CH_3OH_2^+$ (**3**) and $CH_3OH_2^+\cdots OH_2$. The latter structure, being the lowest in potential energy, was therefore taken as the only intermediate, and the reaction scheme:

$$H_2O + CH_3OH_2^+ \rightleftarrows CH_3OH_2^+\cdots OH_2 \rightarrow \text{products} \quad (2)$$

was employed. It was also assumed that the reaction coordinate describing the kinetics of the association/dissociation equilibrium of the first step of this scheme is properly described by the $H\cdots O$ distance. The statistical hypothesis of RRKM theory [3] is an integral part of our μ-VTST treatment. For the present reaction this may be wrong, because trajectory calculations of Hase and co-workers [17] have shown that nonstatistical behaviour because of mode specific behaviour and recrossing of the chemical barrier is found for closely related reactions, exemplified by:

$$Cl^- + CH_3Cl \rightarrow ClCH_3 + Cl^- \quad (3)$$

The only reasonable conclusion to be drawn by these considerations is that a more detailed kinetic treatment is needed in order to compare the probably very accurate CCSD(T) model with the experimental rate constant.

3.2. Clusters

In order to model the effect of the water solvent, calculations were performed for reaction 1 in the presence of an increasing number of water molecules, according to the general reaction scheme:

$$(H_2O)_{n-1}[H_2O\cdots CH_3OH_2^+](H_2O)_{m-1}$$
$$\rightarrow (H_2O)_{n-1}[{}^+H_2OCH_3\cdots OH_2](H_2O)_{m-1} \quad (4)$$

In the following discussion the symbol (n,m) designates a cluster with a given number, $n + m$, of waters. For example, the symbol (1,1) corresponds to the gas phase (no extra waters). The results are given in Table 2 and Figs. 2 and 3.

From these data we discover that the activation energies increase smoothly along the series (1,1), (2,2), (3,3). This is in accord with our expectations, because the dipole moment of the transition structure, $H_2O\cdots CH_3^+\cdots OH_2$ (**ts(3 → 3′)**), of reaction 1 is practically zero, and that of the reactant, $H_2O\cdots CH_3OH_2^+$ (**3**), is quite significant. In a polar medium this leads to better "solvation" of the reactant than the transition structure. Although we cannot be absolutely sure that the smooth transformation of the E_a values with the number of water molecules persist continuously up to $n = \infty$, it seems very likely from the trend discovered for the small clusters.

This assumption is further confirmed because the results for the "unsymmetrical" cluster systems (1,2) and (2,3) fit nicely in between those of the symmetrical (1,1) and (2,2), and (2,2) and (3,3). This is

Table 2
Results of the quantum chemical calculations (MP2/6-31G(d)) for the substitution reactions in water clusters

Molecule	Structure	Energy [a] Hartrees	$\nu^{\#}$ [b] $\mathbf{i} \cdot cm^{-1}$	E_{rel} [c] kJ mol^{-1}	E_{solv} [d] kJ mol^{-1}
H_2O	**1**	−76.176 10	...	...	...
$CH_3OH_2^+$	**2**	−115.582 54	...	...	...
$H_2O\cdots CH_3OH_2^+$, complex (1,1)	**3**	−191.777 75	...	0	50.2
$[H_2O\cdots CH_3\cdots OH_2]^+$, ts (1,1)	**ts(3 → 3′)**	−191.761 52	499	42.6	7.6
$(H_2O)[H_2O\cdots CH_3OH_2^+]$, complex (2,1)	**4**	−267.971 78	...	69.5	97.3
$[H_2O\cdots CH_3OH_2^+](H_2O)$, complex (1,2)	**5**	−267.998 24	...	0	166.8
$(H_2O)[H_2O\cdots CH_3^+\cdots OH_2]$, ts (2,1)/(1,2)	**ts(4 → 5)**	−267.963 71	487	90.7	76.1
$(H_2O)[H_2O\cdots CH_3OH_2^+](H_2O)$, complex (2,2)	**6**	−344.190 22	...	0	208.5
$(H_2O)[H_2O\cdots CH_3^+\cdots OH_2](H_2O)$, ts (2,2)	**ts(6 → 6′)**	−344.167 74	532	59.0	149.5
$(H_2O)_2[H_2O\cdots CH_3OH_2^+](H_2O)$, complex (3,2)	**7**	−420.379 42	...	55.6	242.9
$(H_2O)[H_2O\cdots CH_3OH_2^+](H_2O)_2$, complex (2,3)	**8**	−420.400 57	...	0	298.5
$(H_2O)_2[H_2O\cdots CH_3^+\cdots OH_2](H_2O)$, ts (3,2)/(2,3)	**ts(7 → 8)**	−420.365 35	519	92.5	206.0
$(H_2O)_2[H_2O\cdots CH_3OH_2^+](H_2O)_2$, complex (3,3)	**9**	−496.588 20	...	0	328.8
$(H_2O)_2[H_2O\cdots CH_3^+\cdots OH_2](H_2O)_2$, ts (3,3)	**ts(9 → 9′)**	−496.562 97	535	66.2	262.7
$(H_2O)_2[H_2O\cdots CH_3OH_2^+](H_2O)_2$, complex (in ε)[e]	**9s**	−496.692 76	...	0	(603.5)
$(H_2O)_2[H_2O\cdots CH_3^+\cdots OH_2](H_2O)_2$, ts (in ε)[e]	**ts(9 → 9′)s**	−496.657 15	...	93.5	(510.1)

[a] Including scaled zpve.
[b] Imaginary frequency of vibration, corresponding to displacement in the direction of the reaction coordinate.
[c] For each cluster, (n,m), this is the energy relative to the structure of lowest energy.
[d] Energy relative to that of $CH_3OH_2^+ + (n + m - 1)H_2O$.
[e] PCM calculation (see Secs. 2 and 3.3 for details) performed with the geometry of structure **9** and **ts(9 → 9′)**, respectively.

demonstrated by application of the Marcus theory [18] expression for the activation energy, E_a:

$$E_a(n,m) = E_a^0(n,m)\{1 + [(E(n,m) - E(m,n)] \times [/4E_a^0(n,m)]\}^2 \quad (5)$$

where $E_a^0(n,m) = [E_a^0(n,n) + E_a^0(m,m)]/2$, and $E(n,m)$ and $E(m,n)$ is the energy of the reactant and the product, respectively, of Eq. (3). Note that the way Eq. (5) is applied here implies that the reactions formally are written as already indicated (**4** → **5** and **7** → **8**). From the data of Table 2 we find that $E_a(1,2) = 90.7$ kJ mol^{-1} and $E_a(2,3) = 92.5$ kJ mol^{-1}. From Eq. (5) we get $E_a(1,2) = 91.5$ kJ mol^{-1} and $E_a(2,3) = 93.5$ kJ mol^{-1}, which are in good agreement.

Marcus theory also applies to the geometry of the transition structures. The progress variable (the position of the TS; $\alpha = 0$ for reactant, $\alpha = 1$ for product) is given by:

$$\alpha(n,m) = 0.5 + [E(n,m) - E(m,n)][/8E_a^0(n,m)] \quad (6)$$

For a symmetrical reaction, $\alpha = 0.5$, so for convenience we introduce a variable $\delta = \alpha - 0.5$ to describe the displacement from symmetry for unsymmetrical reactions. In analogy with Fig. 1 we now define a geometrical variable $s = (r^{\#1} - r^{\#2})/(r^{\#1} + r^{\#2})$. It turns out that the actual position of the transition structures (**ts(4 → 5)** and **ts(7 → 8)**) are predicted using Eq. (6) to be within a few percent of the actual values, in that $\delta(1,2)/\delta(2,3) = s(1,2)/s(2,3) = 1.36$.

3.3. Solution

Two conceptually different approaches may be used to model solvent effects in ab initio calculations: (1) In the super-molecule approach a cluster model of the reaction system is investigated, as in the previous section. Provided that the cluster is sufficiently large the results can give realistic results. The main problem is that convergence in the solution energy with size is slow. (2) In the self consistent reaction field approach the reacting unit is embedded in a dielectric

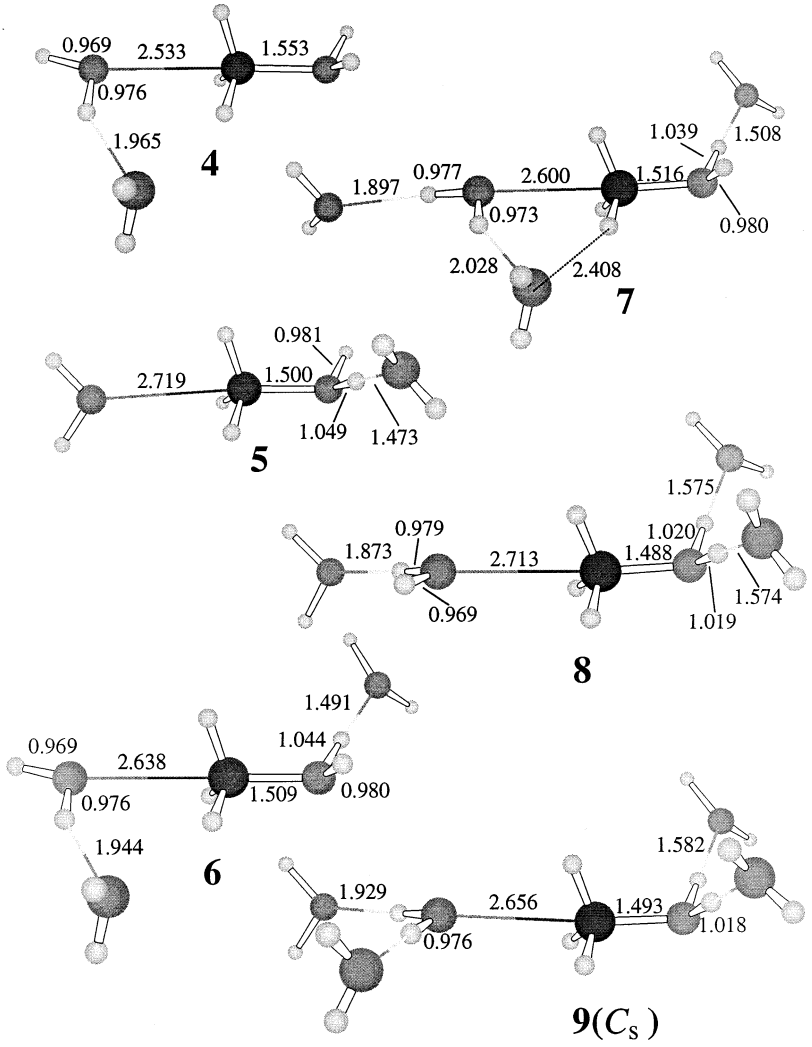

Fig. 2. Geometrical structures of stable reactant and product cluster structures calculated with MP2/6-31G(d). Bond distances are given *i* units of Å.

continuum, and the interaction between the solvent molecules and the reacting unit is treated using perturbation theory. The limitation of this approach is linked to the strong dependence between the calculated solution energy and the size of the cavity chosen for the reacting molecular system. In an attempt to overcome these problems we have combined the two methods.

Because the interactions between the reacting unit, [H_2O, CH_3, OH_2^+], and the water molecules of the first solvation shell are the most important we constructed a super molecule with four extra water molecules, corresponding to the (3,3) cluster. The molecular geometries of the reactant, $(H_2O)_2[H_2O\cdots CH_3OH_2^+](H_2O)_2$ (**9**), and the transition structure, $(H_2O)_2[H_2O\cdots CH_3^+\cdots OH_2](H_2O)_2$ (**ts(9 → 9′)**), were taken directly from the MP2/6-31G(d) calculation. These structures were then subject to single point PCM-MP2/6-31G(d) calculations as explained in Sec. 2. The results are given at the bottom of Table 2, and

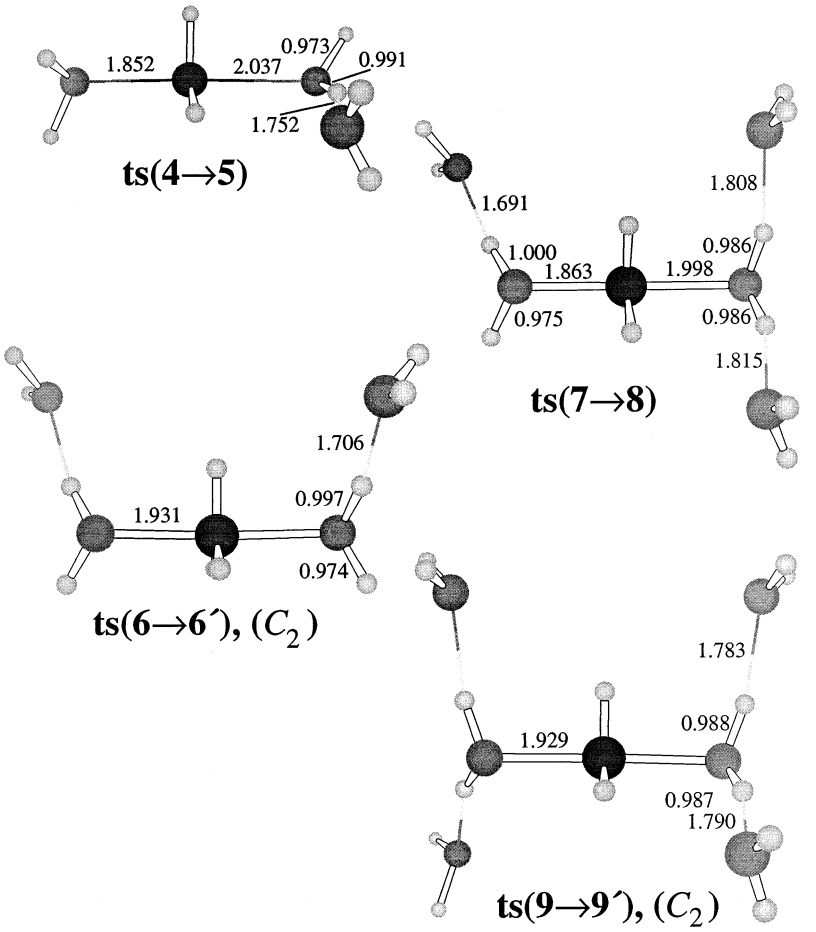

Fig. 3. Geometrical structures of stable transition structures for reactions in the clusters (MP2/6-31G(d)). Bond distances are given *i* units of Å.

an activation energy of E_a = 93.5 kJ mol^{-1} was obtained. A few test calculations were also conducted to monitor the dependence of the cavity size. In these tests the atomic radii were varied by ±0.1 Å relative to their standard values, and the largest deviation was found for hydrogen for which the values were found to vary by ±10%.

Previous experience has shown us that the molecular parameters which determine the height of energy barriers for chemical reactions may be analyzed by appropriate deconstruction of the reactant and the transition structure into the molecular entities they consist of. For this purpose we determined the energetics of the following hypothetical reactions:

$$(H_2O)_{n-1}[H_2O \cdots CH_3OH_2^+](H_2O)_{m-1} \rightarrow CH_3^+ + (H_2O)_n + (H_2O)_m \quad (7)$$

$$(H_2O)_{n-1}[H_2O \cdots CH_3^+ \cdots OH_2](H_2O)_{m-1} \rightarrow CH_3^+ + (H_2O)_n + (H_2O)_m \quad (8)$$

The accompanying dissociation energies, E(RE) and E(TS), respectively, are defined in accordance with these equation. For n,m = 1, 2 and 3 the species H_2O, $(H_2O)_2$ and $(H_2O)_3$ on the right hand sides of

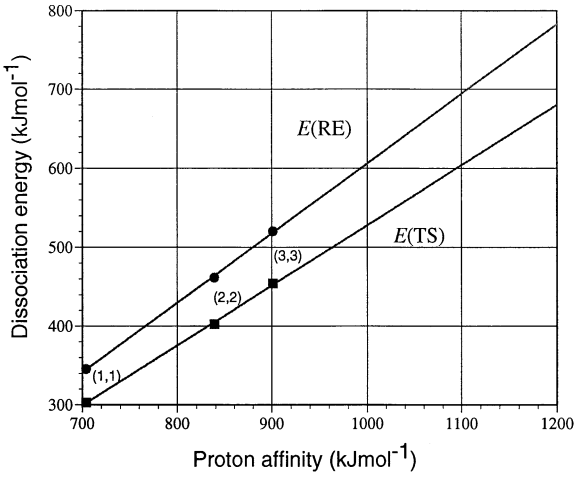

Fig. 4. Plot showing the linear correlation between the quantities E(TS) and E(PR) defined in the text, and the proton affinity (PA) of the corresponding water oligomers.

these equations are the monomer, the dimer and the trimer of water. One slight problem arises because the trimer of water constitutes a cyclic structure with three hydrogen bonds, while there are only two hydrogen bonds within the corresponding moieties in $(H_2O)_{n-1}[H_2O \cdots CH_3OH_2^+](H_2O)_{m-1}$, $(H_2O)_{n-1}[H_2O \cdots CH_3 \cdots OH_2^+](H_2O)_{m-1}$ and $(H_2O)_3H^+$. To solve this problem we have added 21.3 kJ mol^{-1} (equivalent to one hydrogen bond) to the energy of $(H_2O)_3$.

It is well known that the methyl cation affinity of a compound is linearly related to its proton affinity (PA), the ionization energy and related quantities (within a given class of compounds) [19]. In Fig. 4 we have plotted the relationship between the dissociation energies, E(RE) and E(TS), for the (1,1), (2,2) and (3,3) clusters, and the MP2/6-31g(d) proton affinities [6] of the water monomer (704 kJ mol^{-1}), dimer (839 kJ mol^{-1}) and trimer (888 kJ mol^{-1}), respectively. For both E(RE) and E(TS) we find perfect (r = 0.999) linear relationships. This finding is very encouraging, in the sense that the term nucleophilicity in this case can be given a quantitative measure.

In the introduction we raised the question of how well cluster models represent an unbroken line from gas phase to solution phase. In this context the answer is given by further consideration of Fig. 4. The activation energy for a given cluster is given by $E_a = E(\mathrm{RE}) - E(\mathrm{TS})$. The difference between the upper and the lower line of Fig. 4 is (in kJ mol^{-1})

$$E_a = -41.9 + 0.120\ \mathrm{PA} \quad (9)$$

Using this relationship we find that it is possible to extrapolate the linear trend in the activation energies of the small clusters to solution. The proton affinity of bulk water is 1130 kJ mol^{-1} [20], and substitution of this value into Eq. (9) gives E_a = 93.5 kJ mol^{-1}. This is in quantitative agreement with the PCM value, and should therefore be a reliable justification of our extrapolation method. To which extent this value is accurate depends of course on the merits of MP2/6-31G(d) compared to the unknown experimental value and the results of more accurate quantum chemical methods. This will be the subjects of future studies. The apparent linear relationship found between the activation energy and the proton affinity (nucleophilicity) may well be of global validity and will certainly be investigated in greater detail.

Acknowledgements

The author wishes to thank VISTA (The Norwegian Academy for Science and Letters, and Statoil) for financial support and NFR (The Norwegian Research Council) for generous amounts of computer time.

References

[1] G. Giomousis, D.P. Stevenson, J. Chem. Phys. 29 (1958) 294.
[2] D.P. Ridge, in Structure/Reactivity and Thermochemistry of Ions, P. Ausloos, S.G. Lias (Eds.), Reidel, Dordrecht, 1987.
[3] J.I. Steinfeld, J.S. Fransisco, W.L. Hase, Chemical Kinetics and Dynamics, Prentice Hall, Englewood Cliffs, NJ, 1989.
[4] J. Chandrasekhar, S.F. Smith, W. Jorgensen, J. Am. Chem. Soc. 106 (1986) 3049.
[5] D.K. Bohme, A.B. Raksit, J. Am. Chem. Soc. 106 (1984) 3447.
[6] L. Bache-Andreassen, E. Uggerud, Chem. Eur. J., to be published.
[7] M.J. Frisch, G.W. Trucks, H.B. Schlegel, P.M.W. Gill, B.G. Johnson, M.A. Robb, J.R. Cheeseman, T.A. Keith, G.A. Peter-

son, J.A. Mongomery, K. Raghavachari, M.A. Al-Laham, V.G. Zakrzewski, J.V. Ortiz, J.B. Foresman, J. Cioslowski, B.B. Stefanov, A. Nanayakkara, M. Challacombe, C.Y. Peng, P.Y. Ayala, W. Chen, M.W. Wong, J.L. Andres, E.S. Reploge, R. Gomperts, R.L. Martin, D.J. Fox, J.S. Binkley, D.J. Defrees, J. Baker, J.J.P. Stewart, M. Head-Gordon, C. Gonzalez, J.A. Pople, Gaussian Inc., Pittsburgh, PA, 1994.
[8] C.C.J. Roothan, Rev. Mod. Phys. 23 (1951) 69.
[9] A.D. Becke, J. Chem. Phys. 98 (1993) 5648.
[10] R.J. Bartlett, G.D. Purvis, Int. J. Quant. Chem. 14 (1978) 516.
[11] C. Möller, M.S. Plesset, Phys. Rev. 46 (1934) 618.
[12] J. Pople, M. Head-Gordon, K. Raghavachari, J. Chem. Phys. 87 (1987) 5968.
[13] A.P. Scott, L. Radom, J. Phys. Chem. 100 (1996) 16 502.
[14] L.A. Curtiss, K. Raghavachari, G.W. Trucks, J.A. Pople, J. Chem. Phys. 94 (1991) 7221.
[15] S. Miertus, E. Scrocco, J. Tomasi, Chem. Phys. 55 (1981) 117.
[16] S. Miertus, J. Tomasi, Chem. Phys. 65 (1982) 239.
[17] W. Hase, Science 266 (1994) 1994.
[18] R.A. Marcus, J. Phys. Chem. 72 (1968) 891.
[19] T.B. McMahon, P. Kebarle, Can. J. Chem. 63 (1985) 3160.
[20] D.F. Shriver, P.W. Atkins, C.P. Langford, Inorganic Chemistry, Oxford University Press, Oxford, 1990.